Quantum Monte Carlo Simulation of Frustrated Kondo Lattice Models

Toshihiro Sato,[1] Fakher F. Assaad,[1] and Tarun Grover[2]
[1]Institut für Theoretische Physik und Astrophysik, Universität Würzburg, 97074 Würzburg, Germany
[2]Department of Physics, University of California at San Diego, La Jolla, California 92093, USA

(Received 24 November 2017; published 8 March 2018)

The absence of the negative sign problem in quantum Monte Carlo simulations of spin and fermion systems has different origins. World-line based algorithms for spins require positivity of matrix elements whereas auxiliary field approaches for fermions depend on symmetries such as particle-hole symmetry. For negative-sign-free spin and fermionic systems, we show that one can formulate a negative-sign-free auxiliary field quantum Monte Carlo algorithm that allows Kondo coupling of fermions with the spins. Using this general approach, we study a half-filled Kondo lattice model on the honeycomb lattice with geometric frustration. In addition to the conventional Kondo insulator and antiferromagnetically ordered phases, we find a partial Kondo screened state where spins are selectively screened so as to alleviate frustration, and the lattice rotation symmetry is broken nematically.

DOI: 10.1103/PhysRevLett.120.107201

Introduction.—Unconventional, highly entangled states can arise if one starts from a system with a large, perhaps infinite, ground state degeneracy, and then perturb it slightly to lift the degeneracy. Fractional quantum Hall systems clearly fall in this category—at any fractional filling the noninteracting problem of electrons in Landau levels has an infinite number of ground states in the thermodynamic limit. Perturbing this system with interactions leads to a particular superposition of these ground states that corresponds to fractional quantum Hall states. Geometrically frustrated spin systems provide a different class of similar phenomenon. As an example, consider a square lattice where each link ij that connects vertices i, j hosts a spin-1/2 spin $\hat{\boldsymbol{S}}_{i,j}$ which interact via the Hamiltonian $\hat{H}_{\text{classical}} = J\sum_{i,j,k,l\in\square}\hat{S}^z_{ij}\hat{S}^z_{jk}\hat{S}^z_{kl}\hat{S}^z_{li}$. This model has an extensive ground state entropy. Now consider a perturbed model: $\hat{H}_{\text{quantum}} = \hat{H}_{\text{classical}} + \epsilon\hat{S}^x_i$. For nonzero $\epsilon \ll 1$, the ground state of this new model is identical to that of Kitaev's celebrated toric code [1]: it corresponds to an equal weight superposition of the ground states of $\hat{H}_{\text{classical}}$. Motivated by these examples, we ask what phases emerge when a geometrically frustrated spin system is coupled to *fermions*. In this Letter, we will describe a quantum Monte Carlo (QMC) algorithm that allows one to study a large class of frustrated magnets Kondo coupled to fermions, and demonstrate the algorithm by studying a specific model that exhibits new partial Kondo screened (PKS) phases.

For concreteness, consider the following Hamiltonian of interacting fermions and spins, $\hat{H} = \hat{H}_{\text{Spin}} + \hat{H}_{\text{Fermion}} + \hat{H}_{\text{Kondo}}$, where

$$\begin{aligned}
\hat{H}_{\text{Spin}} &= \sum_{i,j}[J^z_{ij}\hat{S}^z_i\hat{S}^z_j + J^{\perp}_{ij}(\hat{S}^+_i\hat{S}^-_j + \text{H.c.})],\\
\hat{H}_{\text{Fermion}} &= \sum_{x,y,\sigma}\hat{c}^{\dagger}_{x\sigma}T_{x,y}\hat{c}_{y\sigma} + \sum_x U\left(\hat{n}_{x,\downarrow} - \frac{1}{2}\right)\left(\hat{n}_{x,\uparrow} - \frac{1}{2}\right),\\
\hat{H}_{\text{Kondo}} &= \sum_{i,x}\frac{J^K_{i,x}}{2}\hat{\boldsymbol{c}}^{\dagger}_x[\sigma^z\cdot\hat{S}^z_i - (-1)^x(\sigma^+\hat{S}^-_i + \sigma^-\hat{S}^+_i)]\hat{\boldsymbol{c}}_x.
\end{aligned} \tag{1}$$

Here the spin 1/2 local moments (electrons) $\hat{\boldsymbol{S}}_i$ $[\hat{\boldsymbol{c}}^{\dagger}_x = (\hat{c}^{\dagger}_{x,\uparrow}, \hat{c}^{\dagger}_{x,\downarrow})]$ reside on a graph with sites labeled by i, j (x, y). J^z_{ij}, $J^{\perp}_{ij}$ defines the potentially frustrated spin model and $T_{x,y}$ the hopping matrix elements of conduction electrons subject to electron correlations modeled by a Hubbard U term [2]. The local moments and electrons interact via the Kondo coupling $J^K_{i,x}$. For the sake of generality we have included the phase factor $(-1)^x$ in the Kondo coupling. This phase factor plays no role if the transverse spin interaction is bipartite, or if the Kondo coupling includes conduction electron only on one sublattice.

It is natural to ask when such Hamiltonians do not suffer from the "sign problem" [3,4], which can make it impossible to simulate quantum systems using finite resources [5]. There are two potential sources of the sign problem: the fermions and the geometrical frustration of spins. Conventionally, these difficulties are tackled in two very different ways. If the fermions were at half-filling on a bipartite lattice, then one can employ a determinantal QMC approach to solve this problem [4,6–8], whereas for spins, if the condition $J^{\perp}_{ij} < 0$ is met (which still allows for geometrical frustration [9,10]), then one can employ a

world-line QMC or stochastic series expansion [3]. Therefore, it is not obvious how one should approach this problem in the presence of the Kondo coupling J^K between the fermions and spins. So far all published studies of frustrated Kondo lattice systems have been limited to nonexact methods, such as mean-filed theory [11], dynamical mean-field theory [12,13], slave-particle mean-field theory [14,15], large-N methods [16,17] and variational Monte Carlo calculations [18–20]. There have also been studies where spins are treated classically [21], and which therefore do not capture the physics of the Kondo screening (i.e., EPR singlet formation between spins and electrons), which is an inherently quantum phenomena. Finally, there has also been progress in simulating a class of models of fermions interacting with geometrically frustrated quantum spins [22–25]. However, the corresponding algorithm is restricted to spin density-density interactions between local moments and electrons, and does not allow for Kondo coupling between spins and fermions.

In this Letter, we will develop an algorithm to solve Hamiltonians of the form in Eq. (1) using QMC calculations when $\hat{H}_{\text{spin}}$ and $\hat{H}_{\text{fermion}}$ are each sign problem-free within bosonic (i.e., $J^{\perp}_{ij} < 0$) and fermionic QMC (i.e., $T_{x,y}$ defines a bipartite graph), respectively. The main innovation is the reformulation of the bosonic problem as a fermionic one by writing spins in terms of Abrikosov fermions [26]: $\hat{\boldsymbol{S}} = \frac{1}{2}\hat{\boldsymbol{f}}^{\dagger}\boldsymbol{\sigma}\hat{\boldsymbol{f}}$, where $\hat{\boldsymbol{f}}^{\dagger} = (\hat{f}^{\dagger}_{\uparrow}, \hat{f}^{\dagger}_{\downarrow})$ is a two-component fermion with the constraint $\hat{\boldsymbol{f}}^{\dagger}\hat{\boldsymbol{f}} = 1$. The constraint is implemented *exactly* by adding Hubbard term $U_f(\hat{f}^{\dagger}_{\uparrow}\hat{f}_{\uparrow} - \frac{1}{2})(\hat{f}^{\dagger}_{\downarrow}\hat{f}_{\downarrow} - \frac{1}{2})$, and taking the limit $U_f \to \infty$. Most importantly, the total $\hat{H}$, including the Kondo coupling $\hat{H}_{\text{Kondo}}$, does not have a sign problem either. This is a consequence of the existence of an antiunitary symmetry under which the Hamiltonian $\hat{H}$ is invariant [27]. The demonstration of the absence of the sign problem builds on Ref. [28,29] and is detailed in the Supplemental Material [30].

The relevance of this class of models to heavy fermion phenomenology alluded above is worth elaborating upon. A simple picture to capture the global phase diagram of heavy fermions was provided by Doniach [31]. For a single impurity Kondo problem, the crossover to the spin-singlet state takes place at the Kondo temperature $T_K = De^{-1/[2N(E_F)J^K]}$, where $N(E_F)$ is the conduction electrons' density of states at the Fermi level E_F, J^K is the exchange interaction between the localized impurity and the conduction electrons, and D is the conduction electrons bandwidth [32]. Now consider a dilute matrix of such local moments. The conduction electrons will mediate long-range RKKY exchange interaction between the local moments whose scale is given by the temperature $T_{\text{RKKY}} \propto (J^K)^2 N(E_F)$. When $T_K \gg T_{\text{RKKY}}$, one obtains the heavy fermion liquid state, which is the many-body analog of the single impurity's spin-singlet ground state. In contrast, in the opposite limit, the spins are likely to order resulting in an antiferromagnetic metal. However, as hinted above, there is a growing list of materials such as CePdAl, $Pr_2Ir_2O_7$, YbAgGe, $YbAl_3C_3$, and Yb_2Pt_2Pb [33–37], where one observes phases which do not easily fit into either of the two limits Doniach considered. The microscopies of these materials suggest that geometrical frustration plays a crucial role in their phenomenology. Therefore, one is motivated to consider a phase diagram where geometrical frustration is an axis in addition to the Kondo coupling.

Case study.—For concreteness, we consider the following model (see Fig. 1):

$$\hat{H}_{\text{Spin}} = J^z \sum_{\langle\langle i,j\rangle\rangle} \hat{S}^z_i \hat{S}^z_j, \qquad \hat{H}_{\text{Fermion}} = -t \sum_{\langle i,j\rangle,\sigma} \hat{c}^{\dagger}_{i\sigma}\hat{c}_{j\sigma},$$
$$\hat{H}_{\text{Kondo}} = J^K \sum_i \frac{1}{2}\hat{\boldsymbol{c}}^{\dagger}_i \boldsymbol{\sigma}\hat{\boldsymbol{c}}_i \cdot \hat{\boldsymbol{S}}_i. \tag{2}$$

In this special case $J^{\perp}_{i,j} = 0$, and the spins and conduction electrons reside on the same honeycomb lattice so that we can use the same indices from spins and conduction electrons. Furthermore, the canonical transformation $\hat{S}^{\pm}_i \to -(-1)^i \hat{S}^{\pm}_i$, $\hat{S}^z_i \to \hat{S}^z_i$ will remove the factor $(-1)^i$ in the Kondo coupling of Eq. (1). $\hat{H}_{\text{Fermion}}$ and $\hat{H}_{\text{Kondo}}$ account for the generic Kondo lattice model on the honeycomb lattice. $\hat{H}_{\text{Spin}}$ is geometrically frustrating since it couples antiferromagnetically local moments on the two underlying triangular Bravais lattices defined on the next-nearest-neighbor sites $\langle\langle i, j\rangle\rangle$ of the honeycomb graph. While this term breaks down the SU(2) total spin symmetry to U(1), time reversal symmetry, essential for the Kondo effect, is present.

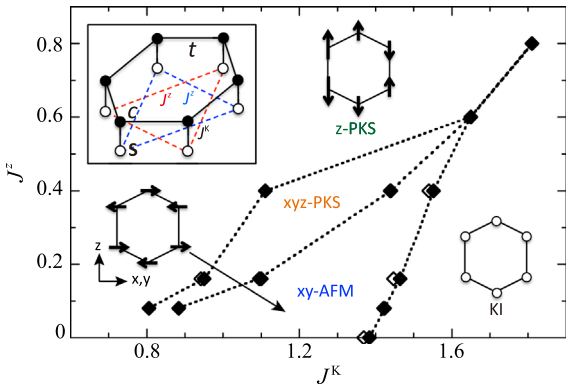

FIG. 1. Phase diagram with in-plane antiferromagnetic (xy-AFM), out-of-plane partial Kondo screening (z-PKS), spin-rotation symmetry breaking partial Kondo screening (xyz-PKS), and Kondo insulator (KI) phases from QMC simulations at $T = 0.025$. Diamonds indicate onset of long-range order; solid (open) symbols are critical values based on $L = 6$ and 9 ($L = 9$ and 12), (see text). Insets: Model and schematic local moment structure in each phase.

For the numerical simulations we used the ALF (Algorithms for Lattice Fermions) implementation [38] of the well-established finite-temperature auxiliary-field QMC method [6,8]. In the Supplemental Material [30], it is shown how to rewrite the model such that it will comply to the data structure of the ALF [38]. We simulated lattices with $L \times L$ unit cells (each containing four orbitals) and periodic boundary conditions. Henceforth, we use $t = 1$ as the energy unit and consider half-filling for the conduction electron. All the data are calculated for temperature $T = 0.025$ (with Trotter discretization $\Delta\tau = 0.1$). In the considered parameter range this choice of temperature is representative of the ground state.

Phase diagram.—Figure 1 shows the phase diagram in the Kondo, J^K, versus frustration, J^z, plane as obtained from a finite-size scaling analysis. To map out the magnetic phase diagram we compute correlation functions of the total spin, $C^\alpha(\boldsymbol{k}) \equiv (1/V)\sum_{\boldsymbol{r},\boldsymbol{r}'}\langle \hat{O}^\alpha_{\boldsymbol{r}}\hat{O}^\alpha_{\boldsymbol{r}'}\rangle e^{i\boldsymbol{k}(\boldsymbol{r}-\boldsymbol{r}')}$, where $\hat{O}^\alpha_{\boldsymbol{r}} = \hat{S}^{\mathrm{tot},\alpha}_{\boldsymbol{r},A} - \hat{S}^{\mathrm{tot},\alpha}_{\boldsymbol{r},B}$ and $\hat{S}^{\mathrm{tot},\alpha}_i = \frac{1}{2}\hat{c}^\dagger_i\sigma^\alpha\hat{c}_i + \hat{S}^\alpha_i$ with $\alpha = (x, y, z)$. Here $\boldsymbol{r}$ labels the unit cell of the honeycomb lattice and A, B the orbitals [39]. We find four phases in the range of parameters shown in Fig. 1. The phase diagram along the $J^z = 0$ axis has been studied earlier [28,29], and reflects the aforementioned competition between RKKY and Kondo screening with an antiferromagnetic (AFM) phase at small J^K, and a Kondo insulator (KI) at large J^K. At J^z precisely equal to zero, the model has an SU(2) symmetry and therefore the AFM order parameter can point in along any direction in the spin space. At infinitesimally small nonzero value of J^z, the spins preferentially order in the x-y plane to minimize the energy cost of geometrical frustration. Hence, this phase is characterized by diverging $C^{x/y}(\boldsymbol{k} = \Gamma)$ and we denote it as xy-AFM in Fig. 1. As the geometrical frustration is increased, the phase diagram changes dramatically. We find two new phases which we denote as z-PKS and xyz-PKS, where the acronym PKS stands for partially Kondo screened. In the z-PKS phase, the U(1) spin rotation symmetry is unbroken while the time reversal symmetry corresponding to the operation $\hat{S}^{\mathrm{tot},z}_i \to -\hat{S}^{\mathrm{tot},z}_i$ is broken. Therefore, this phase is characterized by a diverging $C^z(\boldsymbol{k} = \mathbf{K})$, where $\mathbf{K}$ corresponds the Dirac points of the tight binding conduction electron model. Thereby the z-PKS phase has a $\sqrt{3} \times \sqrt{3}$ unit cell depicted in the inset of Fig. 1. The existence of Kondo screening is crucial to understand the qualitative features of the z-PKS phase, as discussed in detail below. The xyz-PKS phase is a canted version of z-PKS and can be thought of as a hybrid between xy-AFM and z-PKS in that it breaks the symmetries that are broken in either of these phases.

To locate the phase boundaries we consider the renormalization group invariant quantity [40,41]

$$R_\alpha = 1 - \frac{C^\alpha(\boldsymbol{k}_0 + \delta\boldsymbol{k})}{C^\alpha(\boldsymbol{k}_0)}. \tag{3}$$

Here $\boldsymbol{k}_0$ is the ordering wave vector and $\delta\boldsymbol{k}$ the smallest wave vector on the lattice. By definition, $R_\alpha \to 1$ for $L \to \infty$ in the ordered state whereas $R_\alpha \to 0$ in the disordered phase. At the critical point, R_α is scale invariant for sufficiently large L so that results for different system sizes cross. Figures 2(a) and 2(b) show typical results at $J^z = 0.16$. The phase boundaries in Fig. 1 are based on the crossing points of results for $L = 6$, 9 (solid symbols) and $L = 9$, 12 (open symbols), respectively.

The z-PKS phase.—The atomic limit ($t = 0$) reveals aspects of the z-PKS phase. Here the A and B sublattices decouple to form two independent triangular lattices. Translation symmetry breaking of the z-PKS phase leads to a unit cell R for a single sublattice, consisting of three distinct sites n, each accommodating a spin and a conduction electron. A simple variational ansatz for the wave function is the product state $|\Psi_0\rangle = \prod_{R,n}(\alpha_{n,0}|0,0\rangle_{R,n} + \sum_{\mu=-1,0,1}\alpha_{n,\mu}|1,\mu\rangle_{R,n})$, where $|0,0\rangle_{R,n}$, $|1,\mu\rangle_{R,n}$ denote singlet and triplet states of the spin and conduction electrons. The normalization condition $|\boldsymbol{\alpha}_n| = 1$ holds. The variational energy per unit cell takes the form $E = \sum_n(J^K K_n - \frac{3}{32}J^z M_n^2) + \frac{3}{32}J^z(\sum_n M_n)^2$ with $K_n = \langle\Psi_0|\frac{1}{2}\hat{\boldsymbol{c}}^\dagger_{R,n}\boldsymbol{\sigma}\hat{\boldsymbol{c}}_{R,n}\cdot\hat{\boldsymbol{S}}_{R,n}|\Psi_0\rangle$ and $M_n = \langle\Psi_0|\hat{S}^z_{R,n}|\Psi_0\rangle$. As apparent from this form, Kondo screening competes with the geometric frustration [42] and it is energetically favorable to set $\sum_n M_n = 0$. This condition is by no means imposed by symmetries and we have thus checked that our realizations of the z-PKS phase in the QMC simulations indeed satisfy this condition approximately (see the Supplemental Material [30]).

The QMC histogram in the complex plane of

$$\boldsymbol{M}_l = M_{1l}e^{i0} + M_{2l}e^{i(2\pi/3)} + M_{3l}e^{i(4\pi/3)} \tag{4}$$

uniquely reveals the spin structure. Here the additional index l runs over sublattices A and B. Figure 3(a) plots

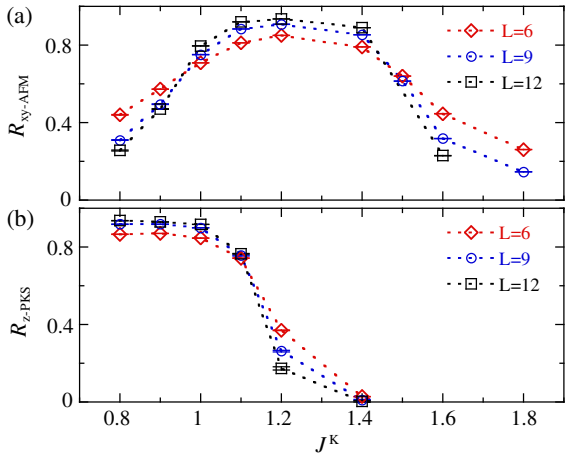

FIG. 2. J^K dependence of correlation ratios for (a) in-plane antiferromagnetic and (b) out-plane three-sublattice orders. Here, $J^z = 0.16$ and $T = 0.025$.

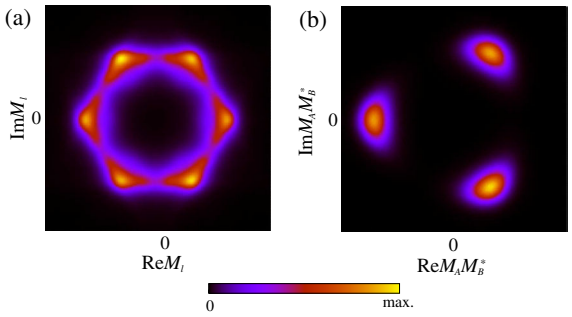

FIG. 3. Probability distribution of (a) $\boldsymbol{M}_l$ and (b) $\boldsymbol{M}_A\boldsymbol{M}_B^*$ for the z-PKS phase at $J^z = 0.60$ and $J^K = 1.5$; see text. Here, $T = 0.025$ and $L = 9$.

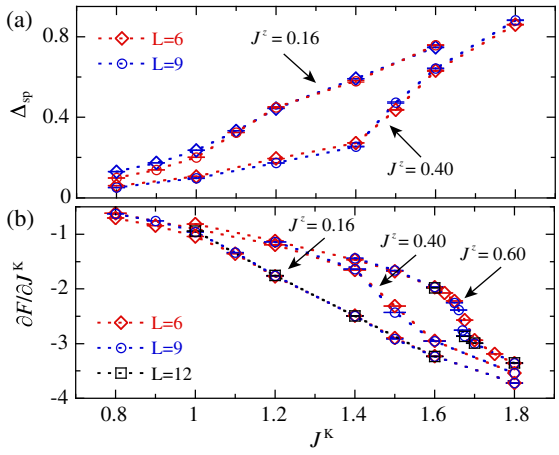

FIG. 4. (a) Single-particle gap Δ_{sp} at the Dirac point [44] and (b) free-energy derivative $\partial F/\partial J^K$. Here, $T = 0.025$.

this quantity, and as detailed in the Supplemental Material [30], corresponds to the sixfold degenerate state $(M_{1A}, M_{2A}, M_{3A}) = \tilde{m}(2, -1, -1)$ and $(M_{1B}, M_{2B}, M_{3B}) = \tilde{m}(-2, 1, 1)$. For example, at $J^z = 0.60$ and $J^K = 1.5$, $\tilde{m} = 0.1$. Away from the atomic limit, the two sublattices couple. The histogram of the quantity $\boldsymbol{M}_A\boldsymbol{M}_B^*$ shown in Fig. 3(b) demonstrates (see the Supplemental Material [30]) that the two sublattices lock-in as depicted in Fig. 1.

Single particle gap.—To set the notation, we write the low energy theory of Dirac fermions on the honeycomb lattice as $\hat{H}_{\text{Dirac}} = \sum_{\boldsymbol{p}} \hat{\Psi}^\dagger(\boldsymbol{p})[p_x\tau^x + p_y\tau^y]\hat{\Psi}(\boldsymbol{p})$ (see Supplemental Material [30] for details). The $\boldsymbol{\tau}$ Pauli matrices act on the sublattice index. The spinors $\hat{\Psi}$ also carry a spin index and a valley index, which are acted upon by the Pauli matrices $\boldsymbol{\sigma}$ and $\boldsymbol{\mu}$, respectively.

In the large J^K limit, one obtains a Kondo insulator, whose ground state may be approximated by a direct product of Kondo singlets between the spin and conduction electron on each site. The single particle gap corresponds to the energy cost of breaking a singlet and is set by J^K [43]. At the mean-field level, the xy-AFM magnetic ordering induces a mass term $M_{x,y} = \langle\hat{\Psi}^\dagger\tau^z\sigma_{x,y}\mu^z\hat{\Psi}\rangle$ of magnitude J^K such that $\Delta_{sp} \propto J^K$. This is consistent with the data at $J^z = 0.16$ shown in Fig. 4. In contrast, the z-PKS phase retains the U(1) spin rotation symmetry but instead breaks time reversal, lattice translation, and point group symmetries. If the sum of the magnetic moments in both sublattices vanishes (i.e., $\sum_m M_m = 0$) then the Dirac points will only shift along the x direction and no single particle gap opens. This is because in the low energy theory such an order parameter corresponds to the term $\hat{\Psi}^\dagger(\boldsymbol{p})\tau^x\sigma^z\hat{\Psi}(\boldsymbol{p})$, which is *not* a Dirac mass since it does not anticommute with the low energy Hamiltonian. However, the Kondo screening is still present in the z-PKS phase as evident by the small value of the magnetic order parameter along the z direction. Therefore, we expect that the mass scale will be set by the Kondo effect and will depend nonperturbatively on J^K as in the single spin Kondo problem. On the other hand, if the condition $\sum_m M_m = 0$ is not satisfied, a mass term proportional to J^K will be generated in the z-PKS phase. As noted earlier, numerically we find that the condition $\sum_m M_m = 0$ is satisfied to a very good approximation. Such a transition from a perturbative to a nonperturbative mass is in qualitative agreement with Fig. 4, where one notices that the single particle gap drops as one enters the PKS phase when increasing the frustration. A precise determination of Δ_{sp} in this phase is difficult since nematicity allows the Dirac points to meander.

Phase transitions.—Figure 4 plots $\partial F/\partial J^K = \langle\frac{1}{2}\hat{\boldsymbol{c}}_i^\dagger\boldsymbol{\sigma}\hat{\boldsymbol{c}}_i \cdot \hat{\boldsymbol{S}}_i\rangle$ along various J^z cuts. We interpret the absence of jump in this quantity in terms of a continuous quantum phase transition. Taking into account time reversal and translation symmetry breaking, the z-PKS phase has a sixfold degeneracy and can be described by an XY model with C_6 anisotropy. C_6 anisotropy is irrelevant at criticality such that the z-PKS phase can be characterized in terms of an effective emergent U(1) symmetry. The xy-AFM phase is characterized by broken U(1) spin symmetry. In the phase diagram of Fig. 1 all phase translation lines are characterized by the spontaneous symmetry breaking of only one of the two aforementioned U(1) symmetries. Thereby we expect all quantum phase transitions to belong to the $(2+1)$D XY universality class.

Summary and discussion.—Using a fermion representation of the spin-1/2 algebra, we have introduced a large class of Kondo lattice models [see Eq. (1)] that are free of the negative sign problem within the auxiliary field QMC approach. Essentially we require the spin system to be free of a sign problem in world-line type approaches and the fermionic system to be particle-hole symmetric such that auxiliary field approaches are equally sign free. This insight gives the possibility of tackling a number of Kondo lattice problems where frustration plays a central role in understanding the phase diagram. It is of experimental relevance since geometrical frustration is present in many heavy fermion materials [33–37].

We have used our approach to compute the phase diagram of the Kondo lattice model on the honeycomb lattice with geometrical frustration, thus adding a new axis in the generic Doniach phase diagram. Aside from the RKKY driven AF order (xy-AFM) with broken U(1) spin symmetry and the Kondo state with the full microscopic symmetries of the model, we observe a novel phase (z-PKS) driven by geometrical frustration. This phase has U(1) spin symmetry but breaks time reversal, lattice, and point group symmetries. It can be understood as a realization of partial Kondo screening in the sense that the strength of Kondo screening becomes site dependent so as to accommodate frustration. As opposed to nonfrustrated models [28,43], the magnetic ordering in the z-PKS phase does not necessarily lead to the opening of a single particle gap. To the best of our knowledge, this is first realization of this type state using approximation-free exact methods. Although our Hamiltonian is not constructed to model a specific material, it is worth noting that a distinct feature of geometrically frustrated heavy-fermion materials such as CePdAl [33] is that similar to the z-PKS phase, they host magnetically ordered phases where the unit cell is enlarged and different sites within a unit cell have a different value of the magnetic order parameter.

We would like to thank M. Raczkowski for fruitful discussions. This work was supported by the German Research Foundation (DFG), Grant No. RA 2990/1-1. The authors gratefully acknowledge the Gauss Gentre for Supercomputing e.V. [46] for funding this project by providing computing time on the GCS Supercomputer SuperMUC at Leibniz Supercomputing Center [47] as well as the John von Neumann Institute for Computing (NIC) for computer resources on the JURECA [48] machine at the Jülich Supercomputing Centre (JSC). T. G. acknowledges support from the UCSD startup funds and is also supported as a Alfred P. Sloan Research Fellow. This work was initiated at the Kavli Institute for Theoretical Physics (KITP) during the program "Entanglement in Strongly-Correlated Quantum Matter" and, correspondingly, this research was supported in part by the National Science Foundation under Grant No. NSF PHY-1125915. We equally acknowledge the Bavaria California Technology Center (BaCaTeC) for financial support.

[1] A. Kitaev, Ann. Phys. (Amsterdam) **303**, 2 (2003).
[2] J. Hubbard, Proc. R. Soc. A **276**, 238 (1963).
[3] P. Henelius and A. W. Sandvik, Phys. Rev. B **62**, 1102 (2000).
[4] E. Y. Loh, J. E. Gubernatis, R. T. Scalettar, S. R. White, D. J. Scalapino, and R. L. Sugar, Phys. Rev. B **41**, 9301 (1990).
[5] M. Troyer and U.-J. Wiese, Phys. Rev. Lett. **94**, 170201 (2005).
[6] R. Blankenbecler, D. J. Scalapino, and R. L. Sugar, Phys. Rev. D **24**, 2278 (1981).
[7] S. R. White, D. J. Scalapino, R. L. Sugar, E. Y. Loh, J. E. Gubernatis, and R. T. Scalettar, Phys. Rev. B **40**, 506 (1989).
[8] F. Assaad and H. Evertz, in *Computational Many-Particle Physics*, Lecture Notes in Physics, edited by H. Fehske, R. Schneider, and A. Weiße (Springer, Berlin Heidelberg, 2008), Vol. 739, p. 277.
[9] R. Moessner and S. L. Sondhi, Phys. Rev. Lett. **86**, 1881 (2001).
[10] S. V. Isakov, M. B. Hastings, and R. G. Melko, Nat. Phys. **7**, 772 (2011).
[11] C. Lacroix, B. Canals, and M. D. Núñez-Regueiro, Phys. Rev. Lett. **77**, 5126 (1996).
[12] Q. Si, Physica (Amsterdam) **378B**, 23 (2006).
[13] M. W. Aulbach, F. F. Assaad, and M. Potthoff, Phys. Rev. B **92**, 235131 (2015).
[14] J. H. Pixley, R. Yu, S. Paschen, and Q. Si, arXiv:1509.02907.
[15] J. H. Pixley, S. Lee, B. Brandom, and S. A. Parameswaran, Phys. Rev. B **96**, 081105 (2017).
[16] P. Coleman and A. H. Nevidomskyy, J. Low Temp. Phys. **161**, 182 (2010).
[17] J. H. Pixley, R. Yu, and Q. Si, Phys. Rev. Lett. **113**, 176402 (2014).
[18] Y. Motome, K. Nakamikawa, Y. Yamaji, and M. Udagawa, Phys. Rev. Lett. **105**, 036403 (2010).
[19] M. Z. Asadzadeh, F. Becca, and M. Fabrizio, Phys. Rev. Lett. **87**, 205144 (2013).
[20] M. Z. Asadzadeh, M. Fabrizio, and F. Becca, Phys. Rev. Lett. **90**, 205113 (2014).
[21] H. Ishizuka and Y. Motome, Phys. Rev. B **88**, 081105 (2013).
[22] Y. Schattner, S. Lederer, S. A. Kivelson, and E. Berg, Phys. Rev. X **6**, 031028 (2016).
[23] Z. H. Liu, X. Y. Xu, Y. Qi, K. Sun, and Z. Y. Meng, arXiv:1706.10004.
[24] F. F. Assaad and T. Grover, Phys. Rev. X **6**, 041049 (2016).
[25] S. Gazit, M. Randeria, and A. Vishwanath, Nat. Phys. **13**, 484 (2017).
[26] A. Abrikosov, Physics **2**, 5 (1965).
[27] C. Wu and S.-C. Zhang, Phys. Rev. B **71**, 155115 (2005).
[28] F. F. Assaad, Phys. Rev. Lett. **83**, 796 (1999).
[29] S. Capponi and F. F. Assaad, Phys. Rev. B **63**, 155114 (2001).
[30] See Supplemental Material at http://link.aps.org/supplemental/10.1103/PhysRevLett.120.107201 for the formulation of the auxiliary field QMC algorithm in Eq. (1) and the z-PKS magnetic ordering.
[31] S. Doniach, Physica B+C (Amsterdam) **91B+C**, 231 (1977).
[32] A. C. Hewson, *The Kondo Problem to Heavy Fermions*, Cambridge Studies in Magnetism (Cambridge University Press, Cambridge, England, 1997).
[33] A. Sakai, S. Lucas, P. Gegenwart, O. Stockert, H. v. Löhneysen, and V. Fritsch, Phys. Rev. B **94**, 220405 (2016).
[34] S. Nakatsuji, Y. Machida, Y. Maeno, T. Tayama, T. Sakakibara, J. van Duijn, L. Balicas, J. N. Millican, R. T.

Macaluso, and J. Y. Chan, Phys. Rev. Lett. **96**, 087204 (2006).
[35] M. S. Kim, M. C. Bennett, and M. C. Aronson, Phys. Rev. B **77**, 144425 (2008).
[36] K. Sengupta, M. K. Forthaus, H. Kubo, K. Katoh, K. Umeo, T. Takabatake, and M. M. Abd-Elmeguid, Phys. Rev. B **81**, 125129 (2010).
[37] Y. Kato, M. Kosaka, H. Nowatari, Y. Saiga, A. Yamada, T. Kobiyama, S. Katano, K. Ohoyama, H. S. Suzuki, N. Aso, and K. Iwasa, J. Phys. Soc. Jpn. **77**, 053701 (2008).
[38] M. Bercx, F. Goth, J. S. Hofmann, and F. F. Assaad, SciPost Phys. **3**, 013 (2017).
[39] We have checked that no instabilities occur in the ferrro-magnetic channel: $\hat{O}^{\alpha}_{\mathbf{r}} = \hat{S}^{\mathrm{tot},\alpha}_{\mathbf{r},A} + \hat{S}^{\mathrm{tot},\alpha}_{\mathbf{r},B}$.
[40] K. Binder, Z. Phys. B **43**, 119 (1981).
[41] S. Pujari, T. C. Lang, G. Murthy, and R. K. Kaul, Phys. Rev. Lett. **117**, 086404 (2016).
[42] Because of the normalization condition, $|\boldsymbol{\alpha}_n| = 1$, finite values of M_m lead to a reduction of the Kondo screening.
[43] H. Tsunetsugu, M. Sigrist, and K. Ueda, Rev. Mod. Phys. **69**, 809 (1997).
[44] The single-particle gap Δ_{sp} is obtained from the asymptotic behavior of the imaginary time single-particle Green function [45].
[45] F. F. Assaad and M. Imada, J. Phys. Soc. Jpn. **65**, 189 (1996).
[46] www.gauss-centre.eu.
[47] www.lrz.de.
[48] Jülich Supercomputing Centre, J. Large-Scale Res. Facilities **2**, A62 (2016).